

# SIMULATION OF INCOMPRESSIBLE FLOW THROUGH RHOMBOHEDRIC PORES

---

---

**Rossella Viola, Ezio Mesini**

---

*Environmental & Mining Engineering, Univ. of Bologna*



ALMA MATER STUDIORUM  
UNIVERSITÀ DI BOLOGNA

**Fabiana Zama**

---

*Dept. of Mathematics, Univ. of Bologna*



ALMA MATER STUDIORUM  
UNIVERSITÀ DI BOLOGNA

**Markus Tuller**

---

*Dept. of Soil, Water and Environmental Science,  
The University of Arizona*



# Introduction

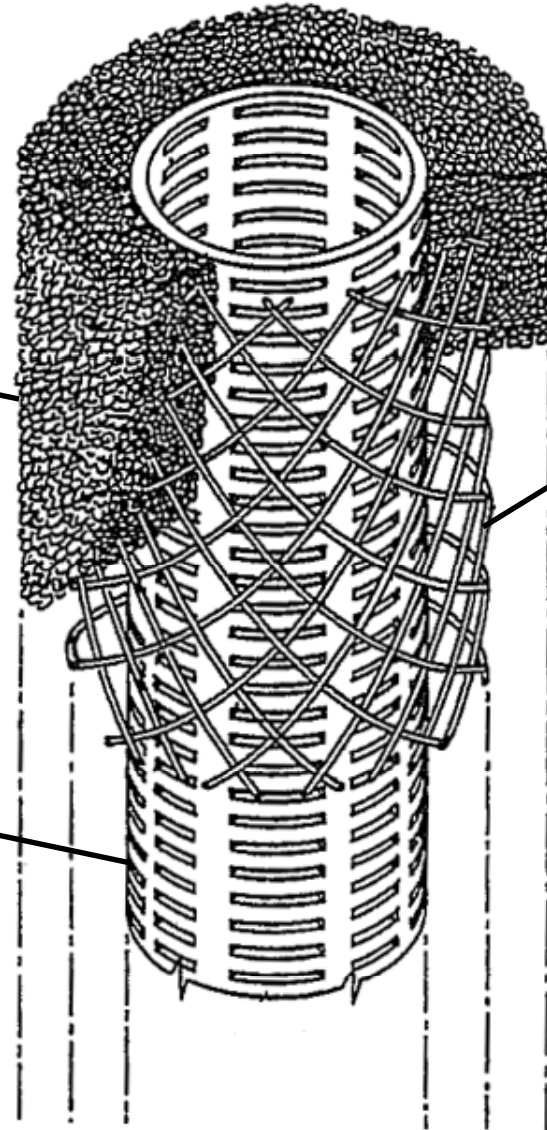
- **Re difficult to define for complex porous media with intricate pore geometries**
- **In packed beds Re calculated based on average pore dimensions is several times lower than for flow through a straight pipe.**
- **Microscopic flow pattern reveal deviations from the linear relationship between pressure drop and flow rate.**
- **Only a few studies focused on three-dimensional (3-D) eddies at the pore-scale, e.g. in a single pore throat between cubic-packed spherical and ellipsoidal grains (1–2 mm diameter).**

# Gravel pack for petroleum or water wells

**Gravel of a predetermined particle size, or mixture of particle sizes**

**Well screen: perforated or slotted pipe**

**Wire cage, as reinforcement**



# aim

To investigate flow through rhombohedric unit pore cells:

- effects of pore geometry on flow behavior, with both water and oil as permeating fluids
- preferential flow paths
- relation between  $Re$  and velocity, pressure gradient and velocity to quantitatively define flow patterns

# Methods- Equations

Numerical simulations in case of laminar flow for a single pore between rhombohedral packed grains (low  $Re < 3$ )

+

3D NAVIER-STOKES equations

$$\rho \mathbf{u} \cdot \nabla \mathbf{u} + \nabla p = \mu \nabla^2 \mathbf{u},$$

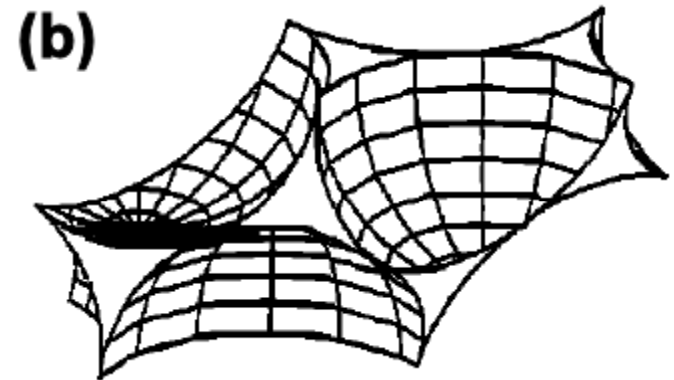
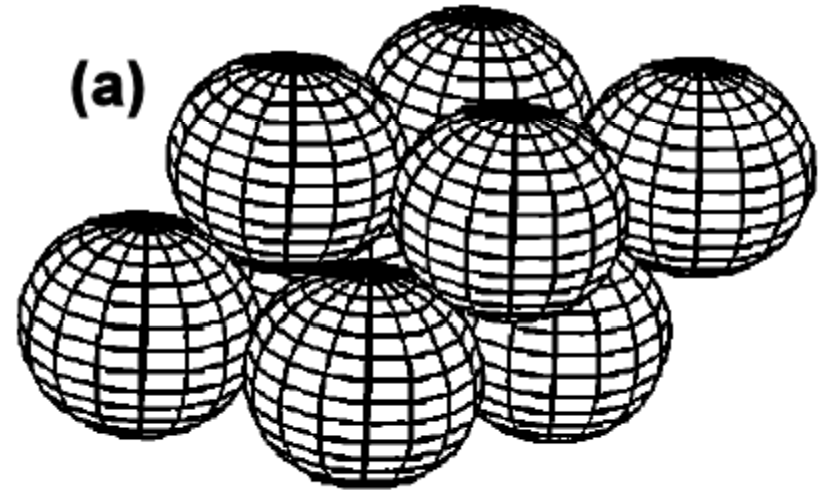
$$\nabla \cdot \mathbf{u} = 0$$

$\rho$  fluid density: 1000(800)  $\text{kg m}^{-3}$ ,

$\mathbf{u} = [u, v, w]$  velocity vector,

$\mu$  dynamic viscosity 0.001(0.01)  $\text{Pa s}$ ,

$p$  total pressure



0.1 mm space between grains  
(1.9-mm diameter)

# Methods-Boundary conditions

- (a) **Wall no-slip ( $u=0$ )** at the grains surfaces.
- (b) **Slip symmetry** at the interfaces between different rhombohedral cells.
- (c) Pressure ( $p = p_0$ ) together with a Dirichlet condition at the inlet surface (defined on the  $(x,y)$  plane at  $z=0$ ) . The condition of no viscous stress was added to assure stability with low Reynolds numbers.

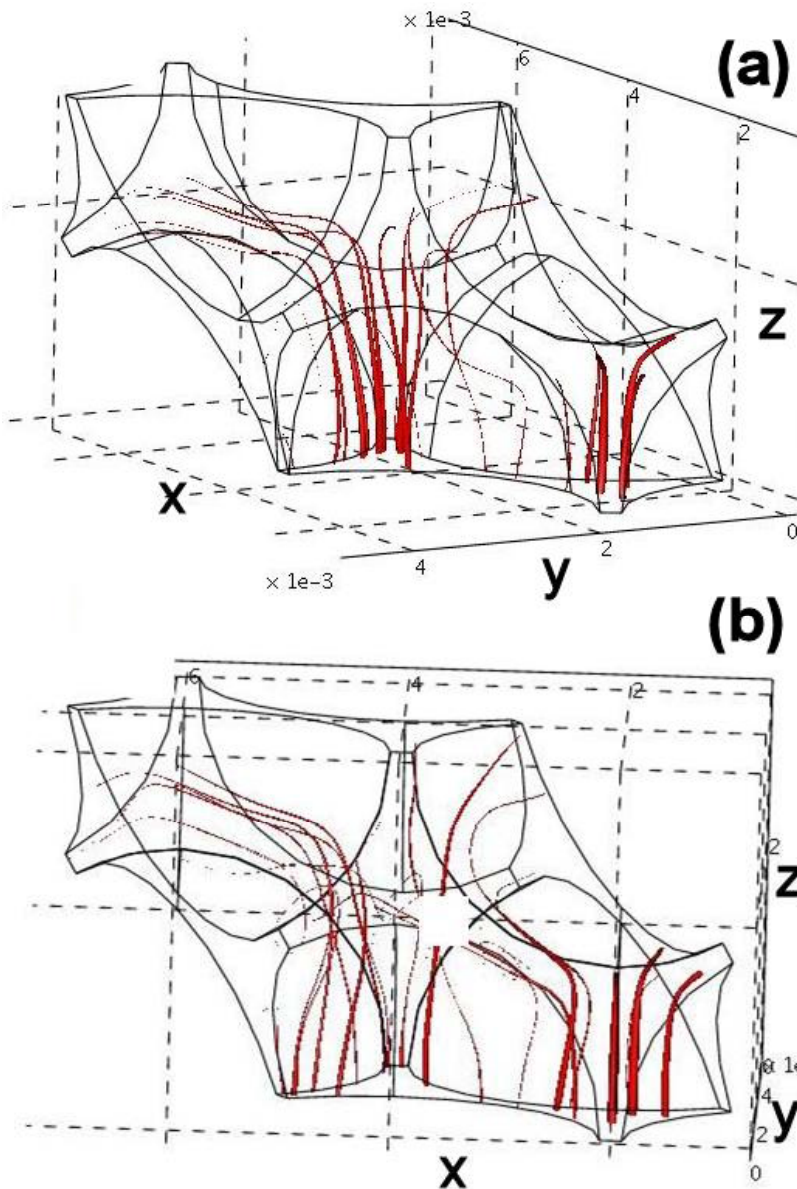
$$(\eta(\nabla u + (\nabla u)^T)n=0) .$$

- (d) Homogeneous pressure ( $p=0$ ) at the outflow surface (defined at  $z=1.E^{-3}$  on the  $(x,y)$  plane).

# Methods- fem solution

- ✓ **1.5E+5 to 5.0E+5 tetrahedral MESH elements.**
- ✓ **Lagrange p2-p1 elements and streamline diffusion (Galerkin least-squares) to assure stability.**
- ✓ **1.E+5 to 4.E+5 Degrees of freedom (DOF)**
- ✓ **Parallel Direct Solver (PARDISO) for small dimension problems; iterative BiCGstab solver coupled with geometric multigrid otherwise.**
- ✓ **In most cases between 4 and 8 iteration steps with the non linear solver for the solution to converge.**
- ✓ **4-processor workstation with 16 GB of shared RAM for computations.**
- ✓ **5 minutes to 1 hour computation times.**

# Results. Streamlines and velocity field



Rhombohedral unit pore cell: inlet pressure at the bottom and zero pressure boundary at outlet faces.

(a) 1 Pa

(b) 5 Pa

Higher velocities can be observed close to grain surfaces, while flow velocities between spheres remain relatively low.

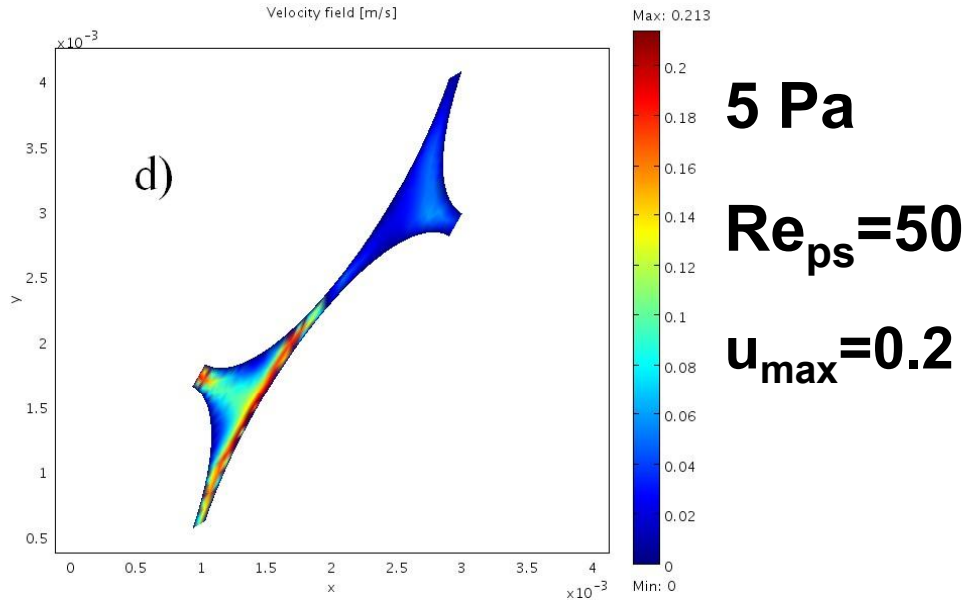
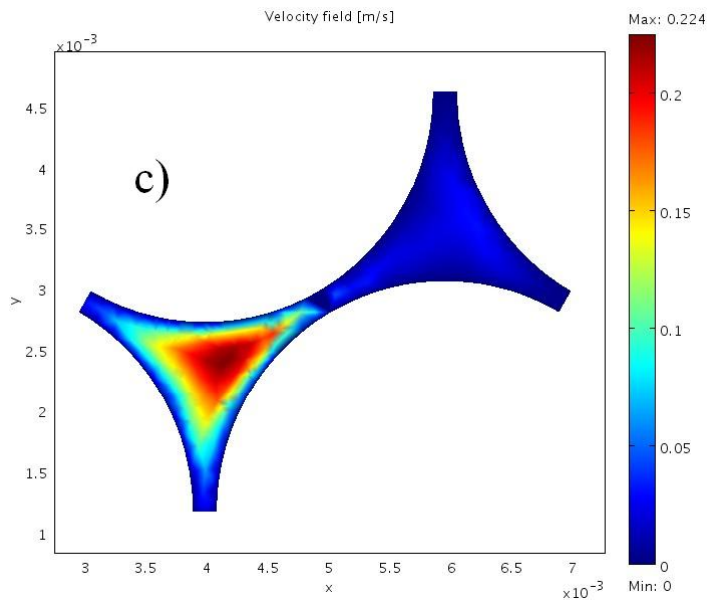
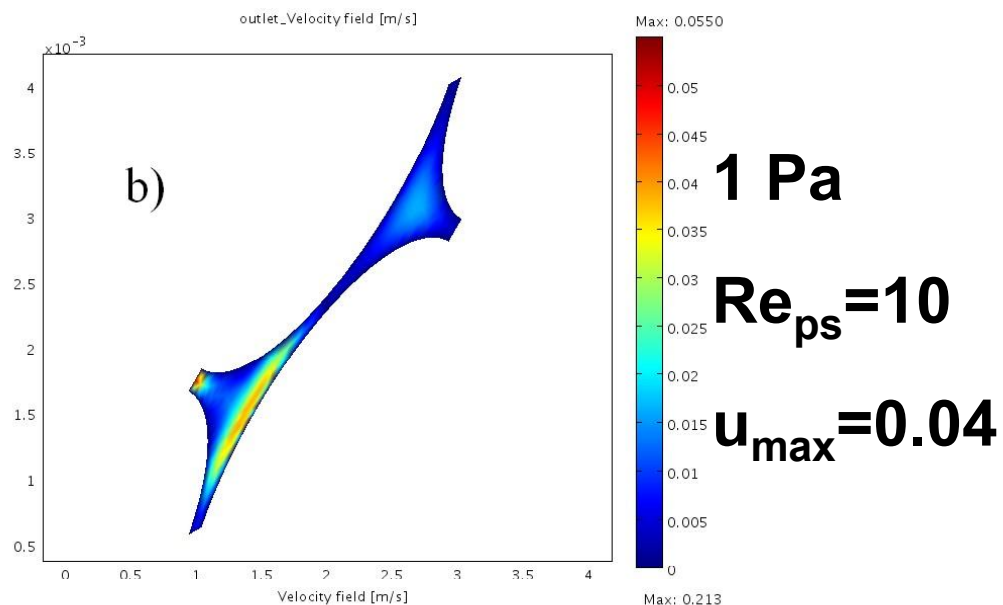
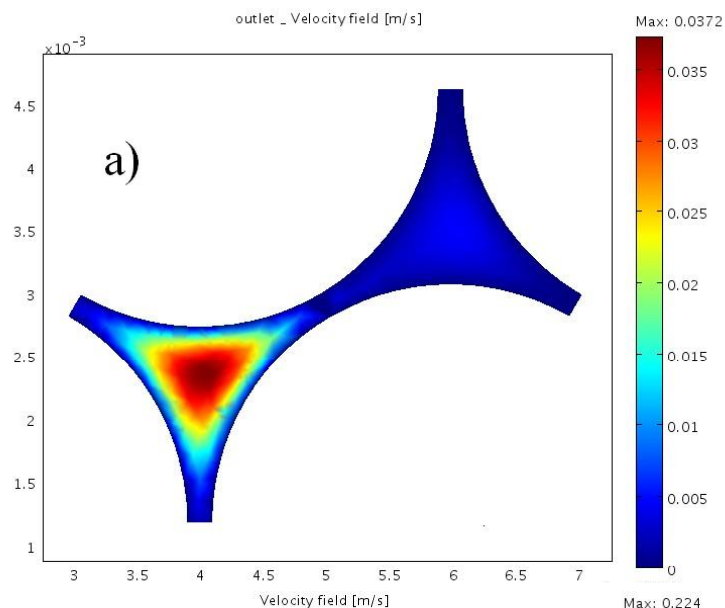
Streamlines reach more distant regions, hence highest velocities occur further away from the solid pore walls.

Evidence of preferred flow paths on the left side of the cell. This is due to the rhombohedral geometry of the pore space with more accessible volume towards the left (path of least resistance).



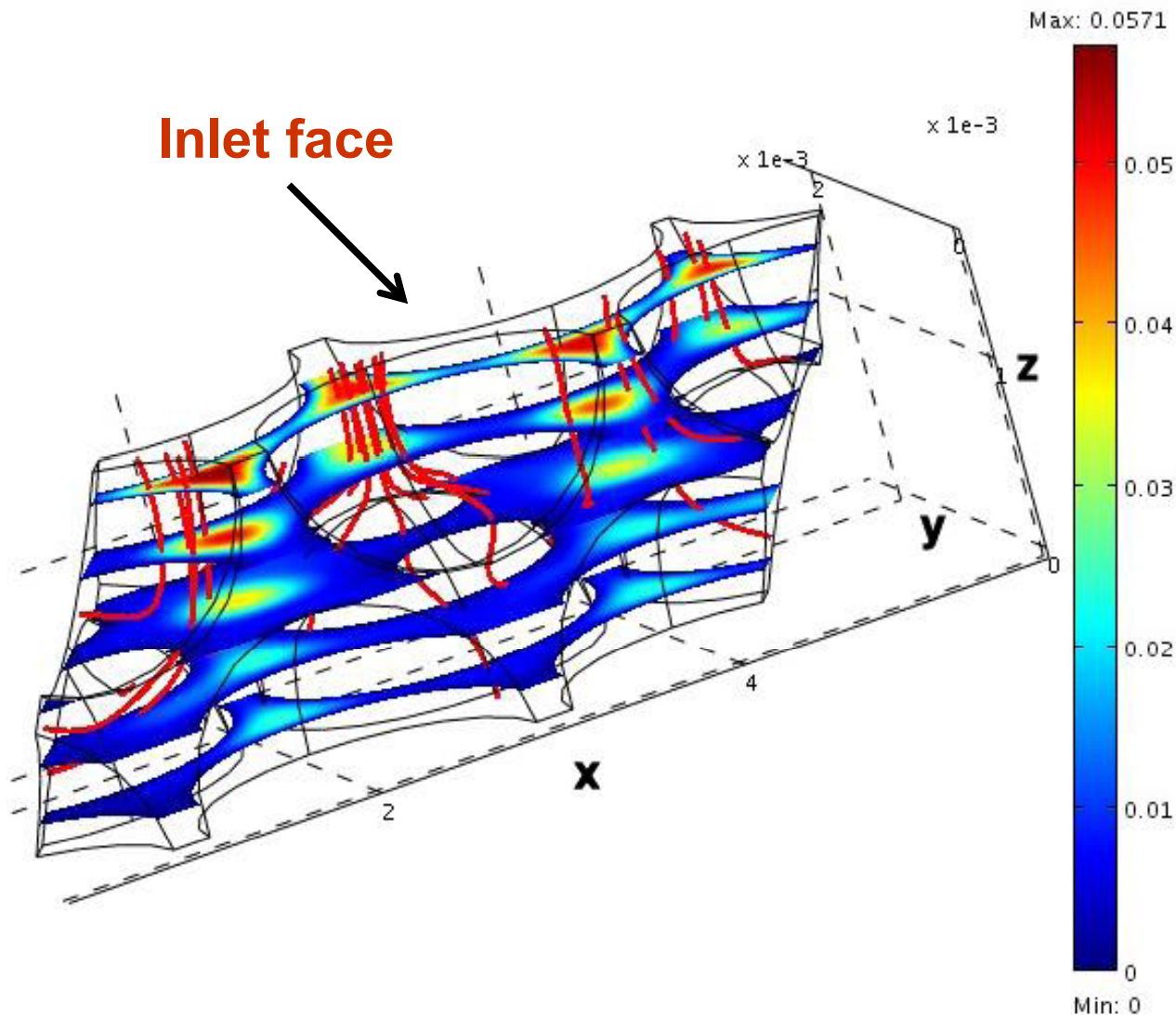
# Results. Pore scale Re and velocity fields

## Outlet faces



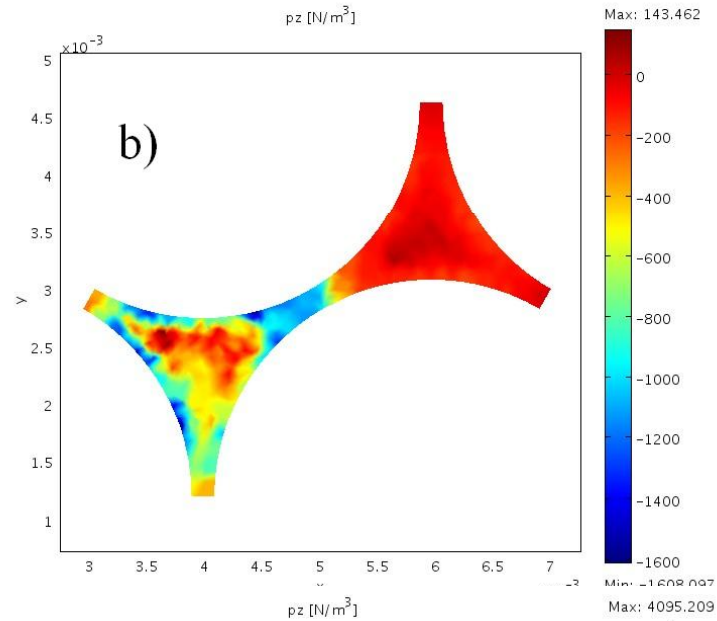
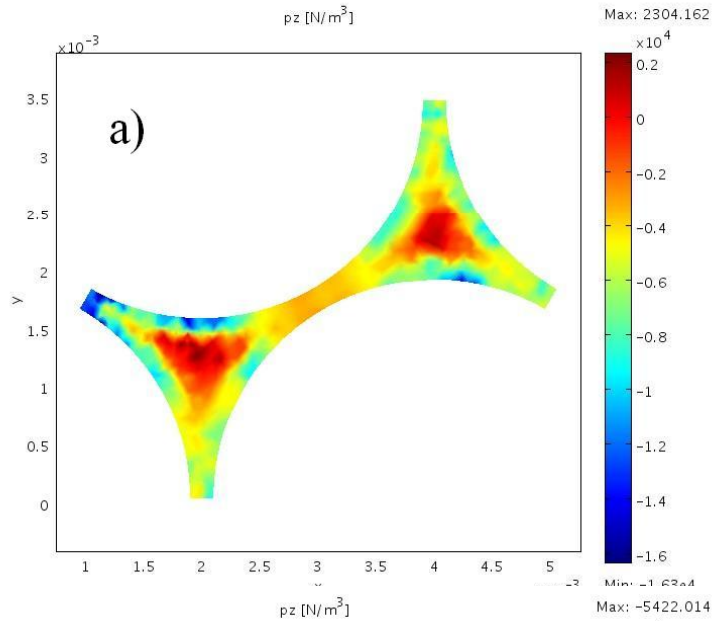
# Results. Pore scale Re and velocity fields

## Two joint rhombohedral cells



**Even for  
this case,  
velocity  
remains  
zero just on  
one side of  
the outlet  
face**

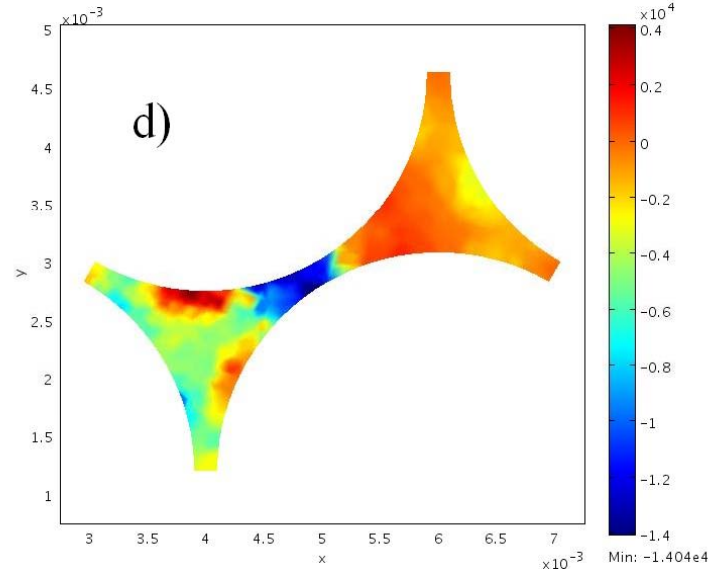
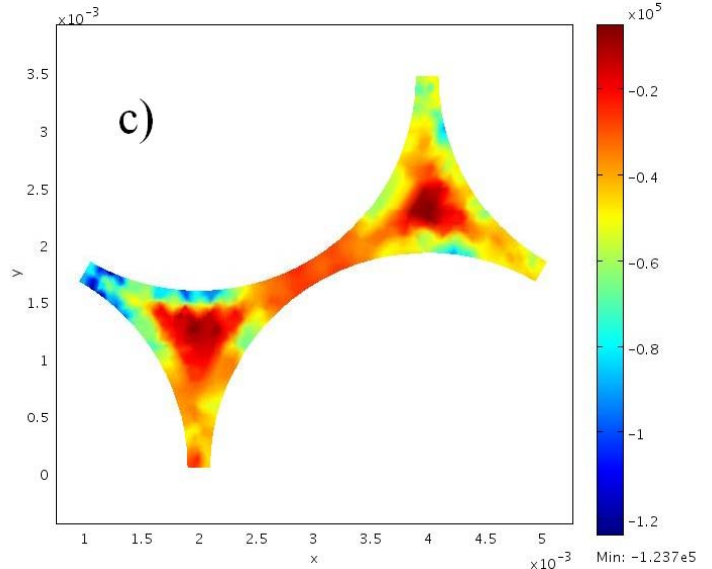
# Results. Pressure gradients



$Re_{ps} = 10$

Inlet (a)

Outlet (b)



$Re_{ps} = 50$

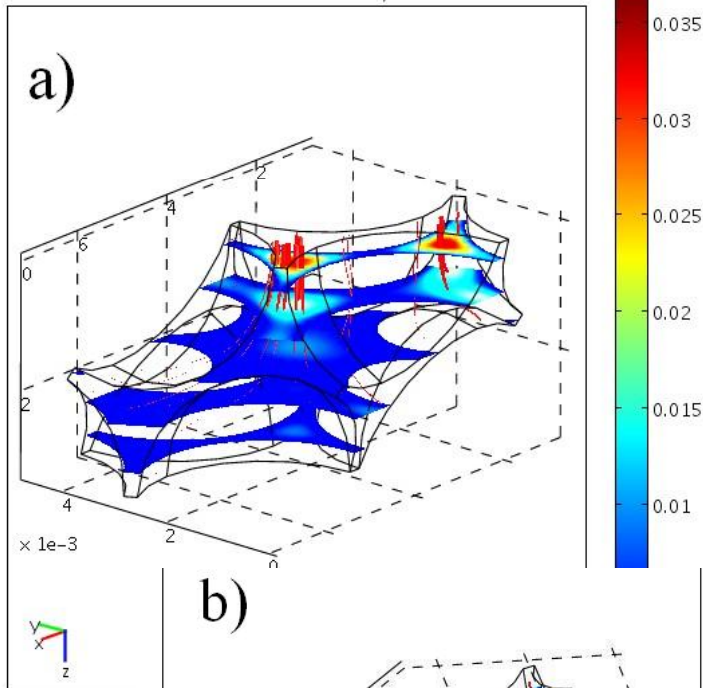
Inlet (c)

Outlet (d)

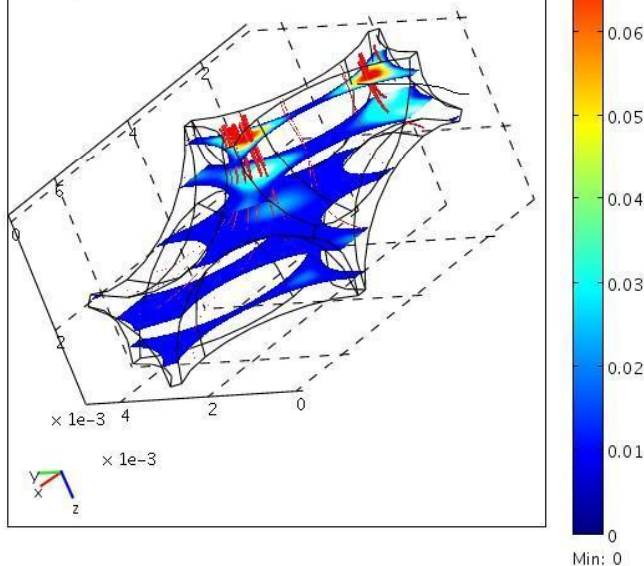
# Results. Case of Oil

Slice: Velocity field [m/s] Streamline: Velocity field  
Streamline Radius: Velocity field

Max: 0.0365

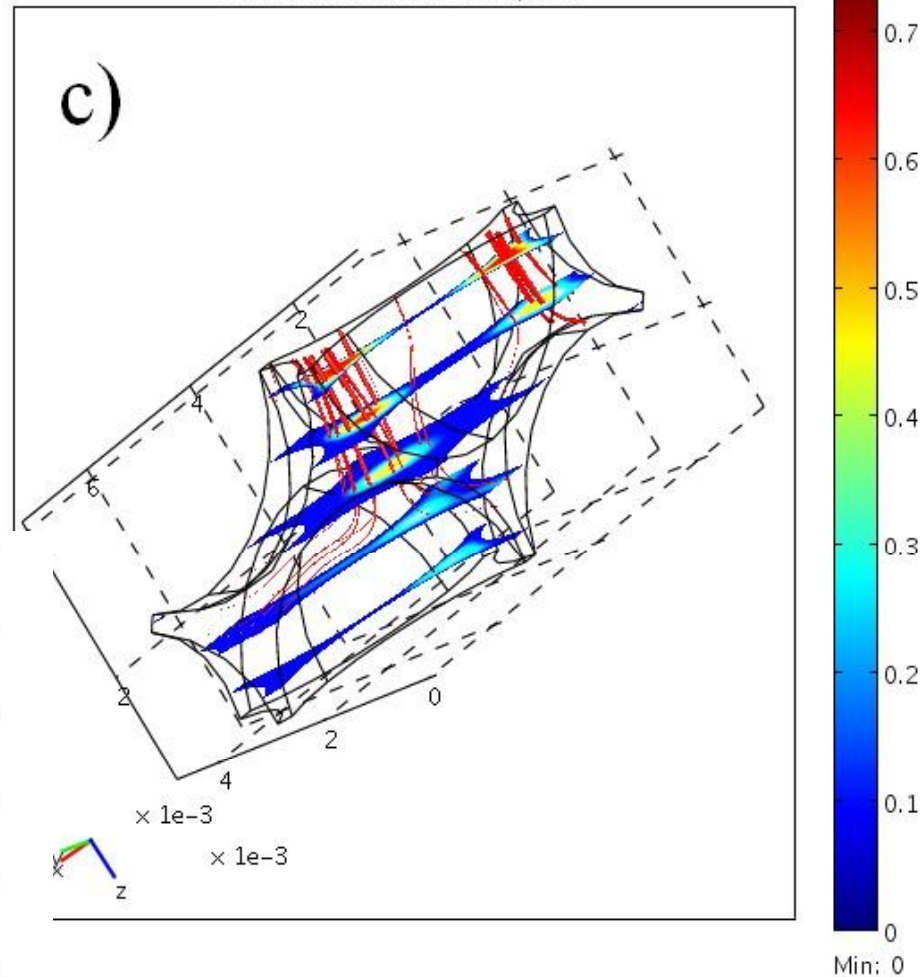


b)



Slice: Velocity field [m/s] Streamline: Velocity field  
Streamline Radius: Velocity field

Max: 0.731



(c) 100 Pa

(a) 5 Pa

(b) 10 Pa

# Conclusions

- **proportionality between gradients and velocities for pore-scale Reynolds numbers ranging from 10 to 50, indicating laminar flow behavior.**
- **preferred flow paths within rhombohedral pores. The presence of a boundary layer near the solid-liquid interface and the development of an inertial core in the center of the pore are visible only on one side of the outlet face. In addition, higher velocity (higher  $Re$ ) is confirmed when the pore-neck and the lateral faces are reached.**

**While for all simulated cases apparent streamline distortion points to inapplicability of Darcy's law, application of incompressible Navier-Stokes equations seems to realistically represent flow phenomena in idealized pore space.**